



# Crashworthiness Performance of Al6061 Tubes with Stiffened Quatrefoil Sections under Axial and Oblique Impact Conditions

İbrahim Kocabaş<sup>1\*</sup>, Haluk Yılmaz<sup>2</sup>

## ABSTRACT

This study presents the crashworthiness performance of Al6061 tubes with stiffened quatrefoil sections under axial and oblique impact conditions. Influences of different types of stiffeners through the depth of tubes in the design of a quatrefoil sectional crash absorber structure are investigated, numerically. Four types of stiffener patterns are considered under oblique impact angles of 0°, 10°, 20°, and 30° measured from the horizontal axis. Force-displacement characteristics, deformation patterns, and crashworthiness indexes of the tested tubes are given to decide optimal crash absorber configuration. The numerical tube models are placed between two rigid plates and an axial impact speed of 1m/s is considered in the numerical study. Al6061 series aluminum alloy is used as a tube material with a multi-linear material model assuming strain-rate independent properties. It is found that the crashworthiness performance is very sensitive to impact angle and Q-S-4 type stiffeners can be proposed for a better tube design.

**Keywords:** Crashworthiness performance, oblique impact, quatrefoil section, stiffener, finite element method

## Güçlendirilmiş Dört Folyo Kesitli Al6061 Tüplerinin Eksenel ve Eğik Darbe Koşulları Altında Çarpışma Dayanıklılık Performansı

### ÖZ

Bu çalışmada, güçlendirilmiş dört-yaprak kesitlere sahip Al6061 boruların eksenel ve eğik darbe koşulları altında çarpışma dayanımı performansı sunulmaktadır. Dört-yaprak kesitli bir darbe sönmüleyici yapının tasarımında boru derinliği boyunca farklı tipte desteklerin etkileri sayısal olarak incelenmiştir. Yatay eksen den ölçülen 0°, 10°, 20° ve 30° eğik darbe açıları altında, dört farklı tipte destek geometrisi incelenmiştir. Test edilen modellerin kuvvet-yer değiştirme karakteristikleri, deformasyon şekilleri ve darbe dayanıklılık indeksleri optimum darbe sönmüleyici konfigürasyonunu belirlemek için kullanılmıştır. Sayısal modeller, iki rijit plaka arasında yerleştirilmiş ve sayısal çalışmada 1m/s'lik bir eksenel çarpma hızı dikkate alınmıştır. Al6061 serisi alüminyum alaşımı, gerinim oranından bağımsız malzeme özellikleri varsayılarak, çoklu-doğrusal malzeme modeli dikkate alınarak boru malzemesi olarak kullanılmıştır. Darbe dayanımı performansının çarpma açısına çok duyarlı olduğu ve daha iyi bir boru tasarımı için Q-S-4 tipi desteklerin önerilebileceği sonucuna varılmıştır.

**Anahtar Kelimeler:** Darbe dayanımı, eğik darbe, dört-yaprak kesit, destek, sonlu elemanlar metodu

\* İletişim Yazarı

Geliş/Received : 13.07.2021

Kabul/Accepted : 20.09.2021

<sup>1</sup> Eskişehir Technical University, Vocational School of Transportation, Eskişehir  
ibrahimkocabas@eskisehir.edu.tr, ORCID: 0000-0003-0600-2034

<sup>2</sup> Eskişehir Technical University, Vocational School of Transportation, Eskişehir  
halukyilmaz@eskisehir.edu.tr, ORCID: 0000-0002-6750-3708

## 1. INTRODUCTION

During the last decade, vehicle safety becomes increasingly important, and more effective crash box systems are being developed for the vehicles, while a growing concern in environmental aspects also requires the design of lightweight structures to reduce fuel consumption. Thus, various novel configurations of structures have been proposed and further improved as energy absorbers during crashes, such as the thin-walled structures, multi-cell tubes, which have been widely studied by the crashworthiness community using analytical, numerical, and experimental methods [1]. These kinds of tubular structures are extensively utilized as energy absorption elements in vehicles such as frontal parts of an automobile chassis, aircraft fuselages, and trains. The major reason is their lightweight properties and high potentials to absorb a great amount of energy during an impact loading to ensure desired occupant protection. Tubular structures are generally responsible for dissipating kinetic energy by undergoing a controlled plastic deformation [2], thus providing passenger safety in case of a crash scenario. For this reason, this kind of passive safety system has a significant role in reducing or completely preventing fatal injuries. Thin-walled structure, as an energy absorber, needs to meet the requirements of structural collapse and deceleration under axial crushing and needs to emerge proper crashworthiness performance under oblique impact loading. This is because that crash-absorbers of the vehicles are also undergone oblique loading conditions in many crashing scenarios.

There are generally two critical parameters to design an optimum crash-absorber, which are geometrical configuration and material of the structure. Material of the energy-absorber structure directly affects the collapse mechanism. Aluminum alloys are generally preferred as an energy absorber material due to their insensitive strain rate-dependent properties for smooth deformation paths at higher crushing speeds. Geometrical configuration plays a more critical role in crashworthiness performance. For this reason, most of the researchers are focusing on the section profiles of the structures. For example, the common tubular sections are circular, polygonal and their derivatives which are investigated by the references [3-5] to improve crashworthiness performance and folding mechanism during crushing. A high amount of energy absorption is a key factor for an ideal crash-absorber structure without extreme initial peak forces (IPF's). For this reason, different corrugated cross-section profiles are generally proposed as an efficient way of controlling structural collapse and folding performance without fracture occurrence of the tube materials [6]. For an ideal energy absorber, the collapse mechanism should be controllable, and the load-displacement diagram should exhibit a plateau as much as possible until the densification region. To perform this task, bio-inspired geometry configurations have been introduced as an alternative method to further improve the crashworthiness performance of the tubular sections. For example, bio-inspired corrugated tubes with different vertex configura-



tions [7] and bio-inspired multi-cell tubes with quadrilateral, hexagonal and octagonal sections [8] are notable studies in this field. Additionally, origami-inspired energy-absorbers structure designs are also used as an effective method to get rid of catastrophic initial peak forces (IPF's) and to get a more smooth force-displacement response. Performances of various origami structures to improve deformation control during axial crushing are presented by ref. [9] and [10].

The above studies of multi-cell structures mainly focus on axial crushing conditions. However, energy absorbers are likely to handle oblique loading conditions in a real vehicle collision. Therefore, the crashworthiness performance of energy-absorbers under oblique loads is attracting attention. For example, Li et al. [11] found that energy absorption of the triangular hierarchical structure under oblique load is considerably higher than that of the non-hierarchical triangular column under axial impact. Tran [12] studied the crumpling of aluminum alloy AA6060-T4 thin-walled tubes subjected to an axial and oblique impact, and it was observed that the crashworthiness performance of the tubes with holes does not improve for both cases of axial and oblique impact. Patel et al. [13] conducted an investigation on homogeneous and heterogeneous ply orientation modeled structure of composite materials under axial and oblique impact loadings to find out suitable model or structure for lightweight vehicle applications. Similarly, Albak [14] performed a study on the crashworthiness performance of twenty-one structures under axial and oblique loading angles. It is reported that subsections added to the inner wall corners of the tubes significantly increase the energy absorption capacity. The section profile and stiffener walls are directly effective on the energy absorption capacity of the tubular structures. Different geometrical sections such as circle, rectangle, and various polygons were examined in terms of energy absorption capacities under oblique impacts to reach an ideal section profile [15]. Furthermore, thin-walled structures with different cross-sections such as circular [16,17], square [18], oblong [19], multi-cell [20,21], multi-corner [22-24], and other unconventional thin-walled structures have already been studied by many researchers. Other complex section tubes have been studied, including star-shaped cross-section [25], convex and concave polygons section [26,27]. Although many geometrical configurations have been studied to improve crashworthiness performance of the crash absorbers, this field is still open to develop a more efficient crash absorber configuration which works well with the oblique impact conditions. In addition, bio-inspired structures, which have been attracting a popularity in recent years, are mostly investigated for only axial-impact conditions. This is an important gap in the literature because a new crash absorber design should be also checked and reinforced for different loading scenarios.

In this paper, the crashworthiness performance of Al6061 tubes with stiffened quatrefoil sections is investigated, numerically under the axial and oblique impact loads. Quatrefoil profile is a special type of bio-inspired geometrical pattern, which exhibits

relatively better crashworthiness performance under axial impact in comparison with the conventional polygonal shapes as a candidate of exterior component of a crash-absorber [28]. To further improve the crashworthiness performance of quatrefoil sections for oblique impact conditions, different stiffener configurations are applied. The influence of four stiffeners arrangements (symmetrically positioned inner ribs inside the quatrefoil tubes) on the crashworthiness performance is examined. In this respect, the present study aims to make a good contribution to the existing state of the field in designing better crash-absorbers that work efficiently with the oblique impact conditions as well.

## 2. MATERIAL METHOD

### 2.1 Crashworthiness Performance Indicators

The efficiency of an energy absorber structure is evaluated through the crucial crashworthiness indicators such as energy absorption (EA), specific energy absorption (SEA), mean crushing force (MCF), initial peak crushing force (IPCF) crushing force efficiency (CFE), and undulation of load-carrying capacity (ULC). The definition of these indicators is as follows:

The energy absorption (EA) is the total deformation energy absorbed during the crushing process. Its formula is expressed as follows:

$$EA = \int_0^L F(x)dx \quad (1)$$

where  $F(x)$  is the instantaneous crushing force at the corresponding crushed length of  $x$  and  $L$  is the stroke length of the crushing process.

The specific energy absorption (SEA), which is defined as the energy absorbed per unit mass of the structure, is utilized to compare the energy absorption capacities of the energy absorbers with different masses as a measure of lightness of the structure. It is calculated by

$$SEA = \frac{EA}{m} \quad (2)$$

where  $m$  is the total mass of the crash absorber.

The mean crushing force (MCF) is one of the important indicators and it is calculated by the ratio of EA to the stroke length  $L$ .

$$MCF = \frac{EA}{L} \quad (3)$$



IPCF is the first reaction induced by the energy-absorbing structure at the beginning of the crushing process. The crushing force efficiency (CFE) is defined as the ratio of MCF related to IPF.

$$CFE = \frac{MCF}{IPCF} \quad (4)$$

The undulation of load-carrying capacity (ULC) displays uniformity of the crushing force versus displacement curve. It is given by

$$ULC = \frac{1}{EA} \int_0^L |F(x) - MCF| dx \quad (5)$$

## 2.2 Geometry of the Tubes

Bio-inspired quatrefoil profile is used as a main section of the crash absorber structure. A schematic illustration of the quatrefoil profile is given in Figure 1. Two geometrical parameters are needed in constructing the quatrefoil profile, which is  $r$  and  $R$  denoting foil radius and outer radius, respectively. Quatrefoil crash absorbers are designed to displace the volume of a cylinder having a diameter and length of 80mm. Stroke length (the length of effective deformation) is chosen as 60mm. In this case, the foil radius  $r$  and outer radius  $R$  are selected to be 20mm and 40mm, respectively. The Wall-thickness of the crash absorber is selected to be 1mm for each configuration.

For axial compression, the quatrefoil sections exhibit relatively better crashworthiness performance as it is mentioned above. However, the crash absorber structure under different oblique impact conditions can lose its efficiency. To improve the efficiency, the use of stiffeners to reinforce the crash absorber leads to an increase in the energy absorption of the structure. To that extent, different stiffener configurations with the

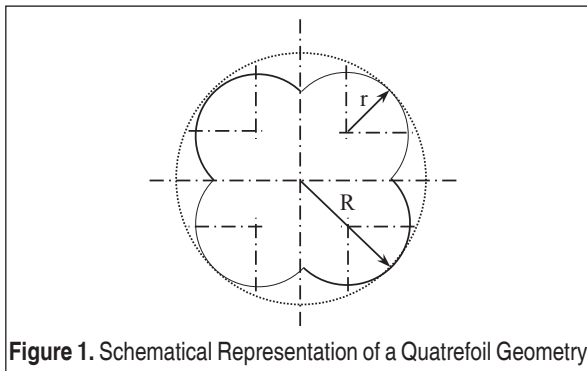
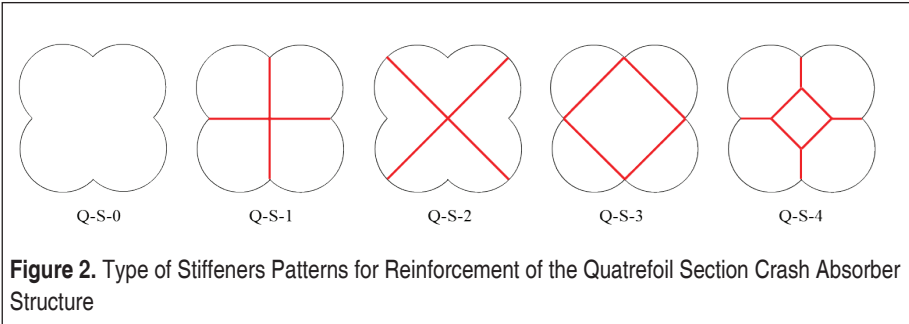


**Figure 1.** Schematical Representation of a Quatrefoil Geometry

same wall thickness are used through the depth of the structure to reinforce empty quatrefoil crash absorber structure. Stiffener patterns are highlighted with the red lines at four different arrangements namely Q-S-1, Q-S-2, Q-S-3, and Q-S-4, (Q denotes quatrefoil, S denotes stiffener, and numbers denote type of stiffener configuration) as can be seen in Figure 2. Q-S-0 represents the empty quatrefoil profile without any stiffener, which can be also used as a reference case for the evaluation of stiffeners influences on crashworthiness performance.



### 2.3 Details of the Numerical Analysis

Numerical simulations are performed using finite element package program ANSYS Workbench employing explicit dynamic solution scheme with AUTODYN solver. Numerical models have meshed with Shell181 four-node quadrilateral shell element with large deformation capability because shell elements are more convenient for

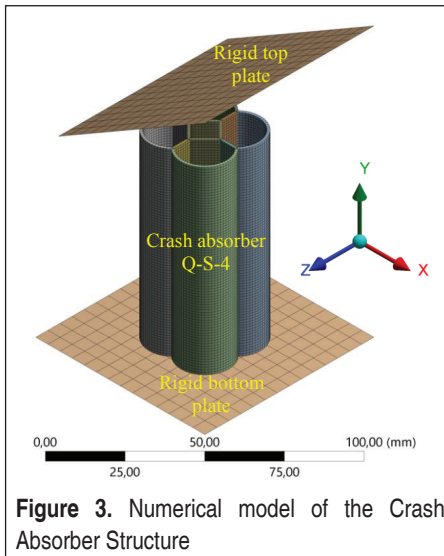


Figure 3. Numerical model of the Crash Absorber Structure

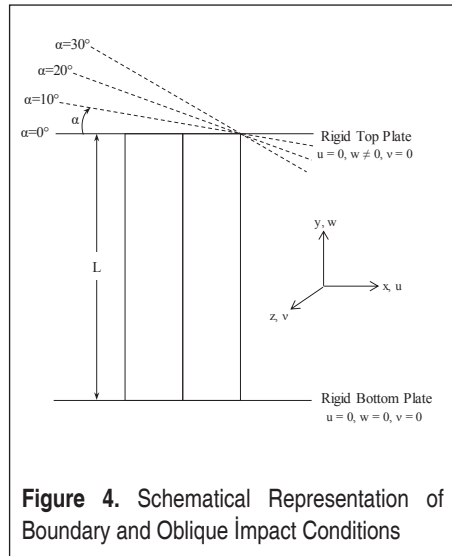
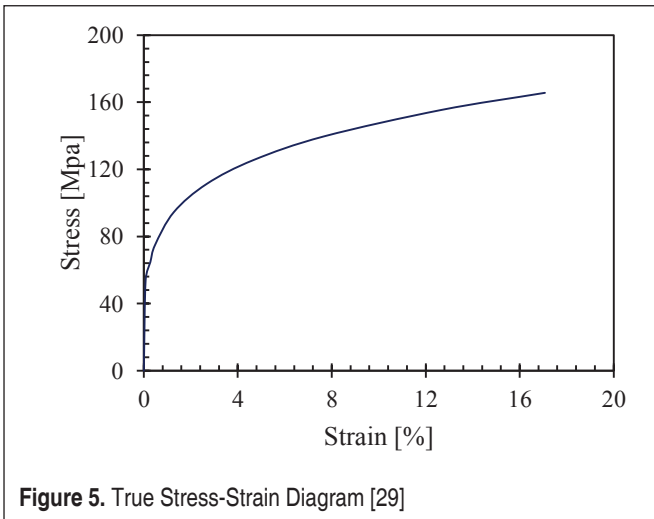


Figure 4. Schematic Representation of Boundary and Oblique Impact Conditions

**Table 1.** Material Properties of AA6061O [29]

Properties	Values
Density $\rho$ (kg/m <sup>3</sup> )	2700
Young's modulus $E$ (GPa)	69.79
Yield stress $\sigma_y$ (MPa)	54
Ultimate stress $\sigma_u$ (MPa)	163.46
Poisson's ratio $\nu$	0.33

thin-walled structures in terms of computational cost. Element edge size is selected to be 1mm, which corresponds 10440, 15328, 17032, 16882 and 16072 element numbers for Q-S-0, Q-S-1, Q-S-2, Q-S-3 and Q-S-4, respectively.

An axial compression with a stroke length of 60 mm is considered. The specimen is placed between two rigid plates (top and bottom plates), as shown in Figure 3 then a speed of 1m/s is applied to the top plate in the axial direction. Boundary and oblique impact conditions are presented in Figure 4. The bottom edge of the crash absorber is bonded to the bottom rigid plate while the penalty contact method (self contact algorithm) is defined at the top with a friction coefficient of 0.15. Four different oblique impact angles which are 0°, 10°, 20°, and 30° are considered.

In the numerical model, the test specimen is modeled with multi-linear plasticity. The material of the crash absorber tube is aluminum alloy, grade AA6061-O, and standard test results of the material are taken from Li et al. [29]. The stress-strain relation is re-

constructed as shown in Figure 5 and the main material properties obtained from the material test are given in Table 1 [29]. Therefore, grade AA6061-O aluminum alloy with the above-mentioned mechanical properties is utilized as a material model for the whole part of the numerical study.

## 2.4 Validation of the Numerical Model

To validate the FE model, experimental test results of the tubes C-S-3 and C-C-3 (the first letter C denotes corrugated, the second letter S denotes square and the second

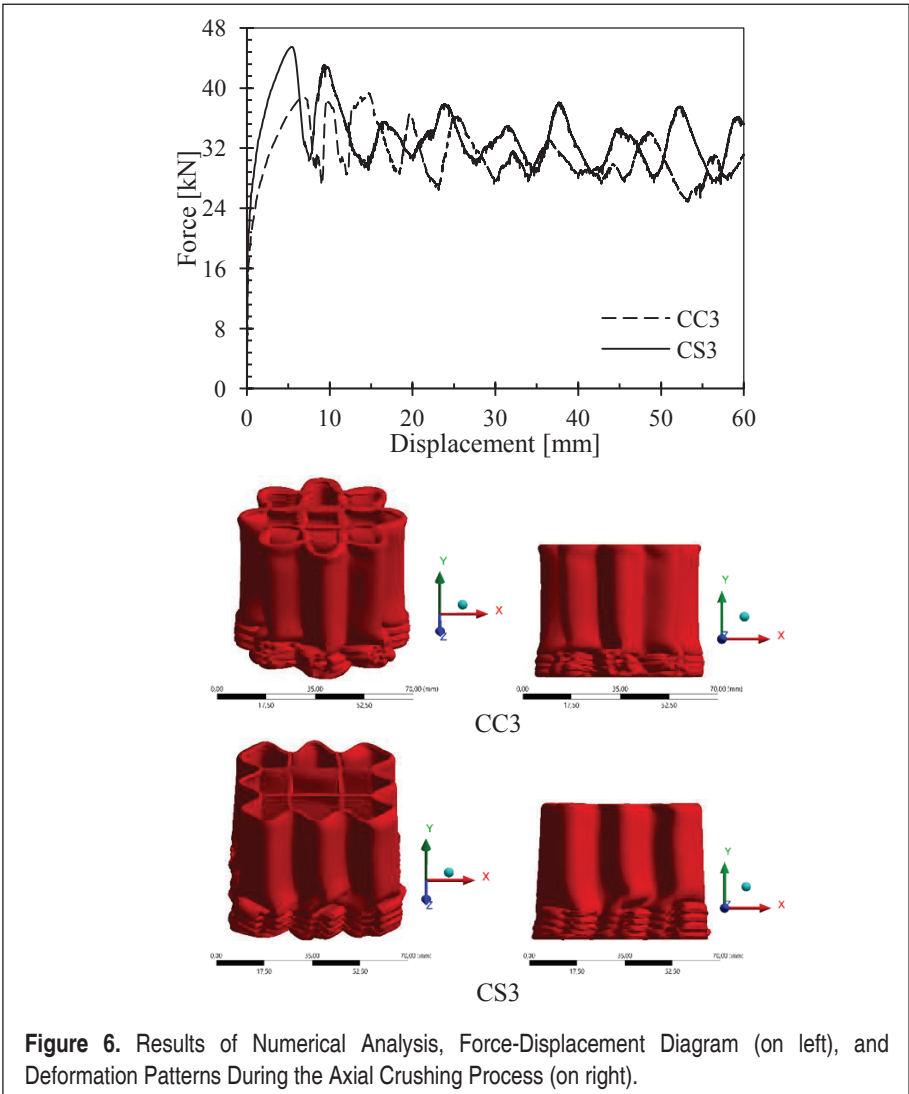




**Table 2.** Comparison of Crashworthiness Performance Indicators Between Referenced Experimental Tests and Numerical Simulations

		IPCF [kN]	MCF [kN]	EA [kJ]	SEA [kJ/kg]	CFE [-]
C-C-3	Test 1	38.74	29.16	1.73	23.72	0.75
	Test 2	37.75	28.24	1.69	22.91	0.75
	Present Study	39.31	30.63	1.86	25.25	0.78
	Mean Error [%]	2.78	6.72	8.77	8.30	3.89
C-S-3	Test 1	44.35	31.99	1.92	20.85	0.72
	Test 2	44.00	31.00	1.86	20.17	0.70
	Present Study	45.46	33.2	2.02	21.91	0.73
	Mean Error [%]	2.91	5.41	6.88	6.83	2.86

letter C denotes circular, the number denotes order of corrugation) are used in ref. [29] under quasi-static compression condition. The test specimen has a wall thickness of 1 mm, and a length of 100mm. A detailed description of the reference geometries (C-S-3 and C-C-3) and experimental test conditions can be accessed in the above-cited reference. Results of FE simulation for the C-S-3 and C-C-3 configurations are illustrated in Figure 6. It shows that the axial crushing process (collapse mechanism) and force-displacement curves agree well with the test results in ref. [29].

In addition, the most important crashworthiness performance indicators are also compared. These indicators are IPCF, MCF, EA, SEA, and CFE. These crashworthiness performance indicators are calculated based on the numerical simulation results and are presented in Table 2. In Table 2, two reference test results and numerical study of the present study are given including the above-mentioned crashworthiness indicators. Deviations of each indicator from the average values of the test results in the reference study are considered as a validation tool. It is seen that amount of the mean errors vary in the range of 2.78 and 8.77% for C-C-3 configuration and 2.86 and 6.88 for C-S-3 configuration, as can be seen in Table 2. This validation routine indicates that the numerical model has good proximity with the reference experimental test results and can be used for the investigation of different configurations of the quatrefoil crash absorber structure.

### 3. RESULTS AND DISCUSSION

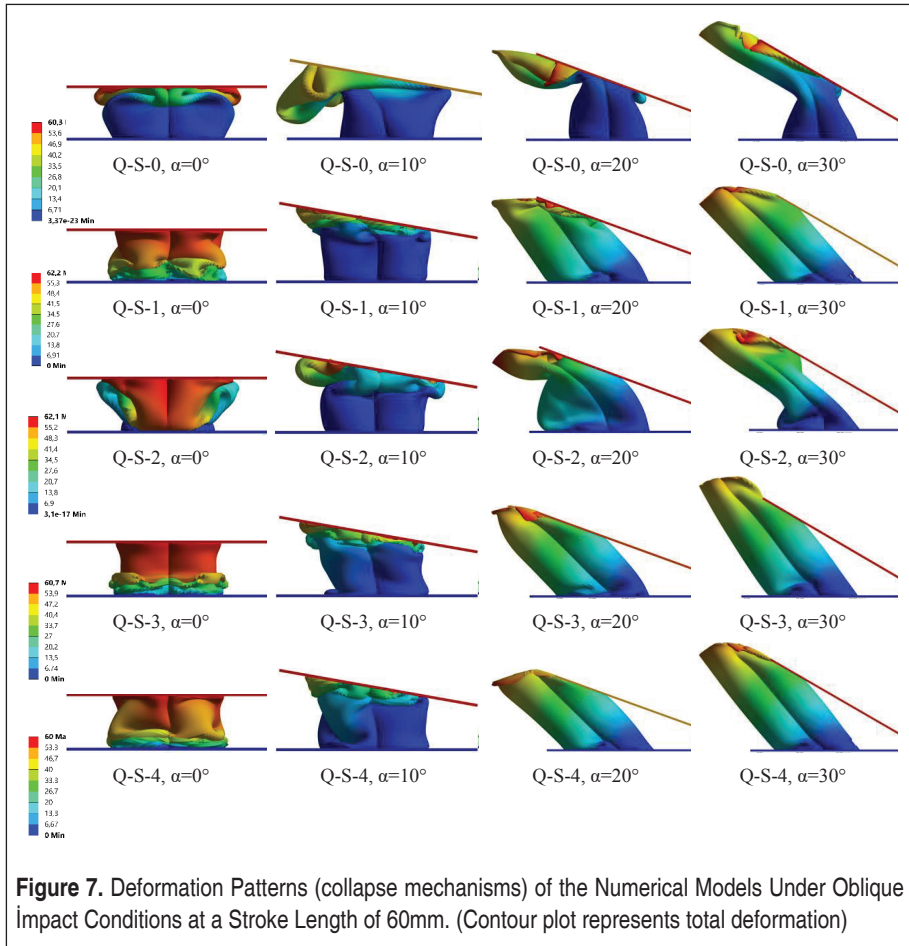
#### 3.1 Crashworthiness Analysis

To emerge the improvement of the crashworthiness performance of the Al6061 tubes

with stiffened quatrefoil sections and to compare different stiffener configurations (thin-walled ribs through the depth of the crash absorber structure), five tubes are simulated under oblique impact conditions. The oblique impact angles measured from the horizontal plane are  $0^\circ$  (referring to axial impact),  $10^\circ$ ,  $20^\circ$ , and  $30^\circ$ . The tubes have the length  $L=80$  mm, and wall thickness  $t = 1$  mm, and all the stiffeners have the same wall thickness of 1mm. The final deformation shapes of these tubes (crash absorber structures) are shown in Figure 7. It is observed that all of the tubes deformed orderly and progressively for axial impact conditions. In all axial impact cases, the tubes deform with the in-extensional mode, which causes more plastic hinges to occur as a result of progressive folding edges.

Crushing energy during an impact loading is generally absorbed with bending deformation and membrane deformation for thin-walled structures. The oblique impact can be considered as an important factor to increase the portion of the bending deformation, and more bending energy is produced in these stiffened tubes. However, the amount of absorbed energy caused by membrane deformation will considerably reduce since the crash absorber structure collapses as a result of catastrophic bending deformation. This leads to a sharp drop in the energy absorption capacity of the structure. Therefore, the implementation of stiffener configuration certainly improves the crush resistance performance of the quatrefoil sections. This conclusion is also confirmed by the deformation patterns of the tubes at the end of the stroke length (total deformed length) of 60mm, as shown in Figure 7. It can be seen that the bending deformation levels of Q-S-n (stiffened sections where n equals 1, 2, 3, and 4) profiles are larger than those of Q-S-0 with the same oblique impact angles. Furthermore, increasing the impact angle induces additional bending deformations in the lateral axis, which nearly causes to disappear the absorbed crashing energy of membrane deformation. For visual details, the deformation patterns corresponding to the impact angles of  $20^\circ$  and  $30^\circ$  can be indicated in Figure 7. This has negative influences on improving the crashworthiness performance of the quatrefoil sections because as the impact angle increases crash absorber structure almost undergoes pure bending deformation. In this case, the progressive folding mechanism is distorted, and the number of plastic hinges decreases throughout the depth of the tube which eventually leads to a greater loss in controlling the plastic deformation mechanism. It is also noteworthy that the oblique impact conditions can exhibit a response that is very similar to a typical buckling behavior. This is more visible in Q-S-0 and Q-S-2 configurations at 30 degrees (see Figure 7), which makes the deformation unstable.

It is pretty better to make a certain evaluation on the force-displacement diagram to reveal the influences of the stiffeners. For this purpose, the typical force-displacement curve of each tube is constructed for the aforementioned oblique impact angles, as can be seen in Figure 8. For an ideal crash absorber, it is desired to have a plateau after IPCF until the densification point at which no extra folding occurs. Secondly, the



deviations in force reaction should be minimized as much as possible. There are also important crashworthiness indexes to extensively compare the crashworthiness characteristics of the considered tubes, and they are mentioned in the following section in detail. Once the force-displacement curves of Q-S-0 (unstiffened tubes) configurations are examined, it is seen that they experience a high amount of deviations for axial impact and 10 degrees of oblique impact conditions. On contrary, a more smooth force-displacement path is observed as the impact angle increases to

20° and 30° with a considerably lower initial peak force (IPF) as can be seen in Figure 9. This is an evidence that the reference Q-S-0 profile is sensitive to oblique impact conditions. On the other hand, the use of cross shape stiffener (Q-S-1) produces greater fluctuations with higher amplitudes, as can be seen in Figure 8 (Q-S-1 config. at 0° and 10°). As the impact angle increases to 20° and 30°, the initial slope of the

force-displacement curves dramatically drops for all the tube configurations because bending deformations become more dominant which eventually causes an excessive drop in load-bearing capacity. Actually, this behavior may be considered as a typical snap-through due to recovery in load-bearing capacity after reaching the maximum value which is mostly experienced in thin-walled structures. However, at lower impact angles (up to  $10^\circ$ ), the stiffeners work well and handle the negative bending effects of the oblique impact condition in comparison with the reference tube (Q-S-0). It does not mean that the stiffeners are ineffective at higher impact angles. For example, Q-S-n series are observed to exhibit nearly similar force-displacement characteristics with almost two times greater load-bearing capacities.

### 3.2 Selection of Ideal Stiffener Structure

There are several crashworthiness performance indicators as mentioned above to select the most appropriate tube configuration as a crash absorber structure. These indicators are IPCF, MCF, SEA, and ULC. Among these indicators, SEA is a key factor which directly represents the energy absorption capacity and lightness of the crash absorber for a given dissipated crushing energy. For this reason, SEA is generally accepted to be the most important parameter for a crash absorber design, and it is also related to the cost criterion. Fairly, a multi-criteria decision-making process must be applied to the results because only one parameter is not adequate to select an ideal structure. A good energy absorber always requires high SEA with a low ULC. Moreover, CFE is expected to be at around unity because high IPCF value produces great instantaneous acceleration threatening occupant protection.

The results of crashworthiness indicators concerning the oblique impact angles of  $0^\circ$  (referring to axial impact),  $10^\circ$ ,  $20^\circ$ , and  $30^\circ$  are shown in Figure 9. For axial impact ( $0^\circ$ ), it can be inferred from Figure 9 that the use of Q-S-4 stiffeners almost exhibited improved values for greater SEA and MCF and also greater IPCF values than the other tube profiles, except for the ULC in Q-S-2, but the two ULC values are still quite close (0.127 for Q-S-4 and 0.101 for Q-S-2). Apparently, Q-S-4 has better crashworthiness performance for axial impact condition since the SEA is always considered to be the most important evaluation criterion for energy absorption structures. Similarly, Q-S-4 is also selected to be the most ideal tube profile with a SEA value of 28.3kJ/kg at an impact angle of  $10^\circ$ . It is also observed that the use of stiffeners in a quatrefoil section provides substantial improvements for all of the indicators under oblique impact conditions, as can be seen in Table 3. However, it can be concluded that the Q-S-1 has better crushing performance than the Q-S-4 under  $20^\circ$  oblique impact. This is because that the Q-S-1 undergoes more plastic deformation than that of the Q-S-4 profile based on the deformation patterns in Figure 7. The comparison between the stiffener configurations is relatively complicated because it can be reported

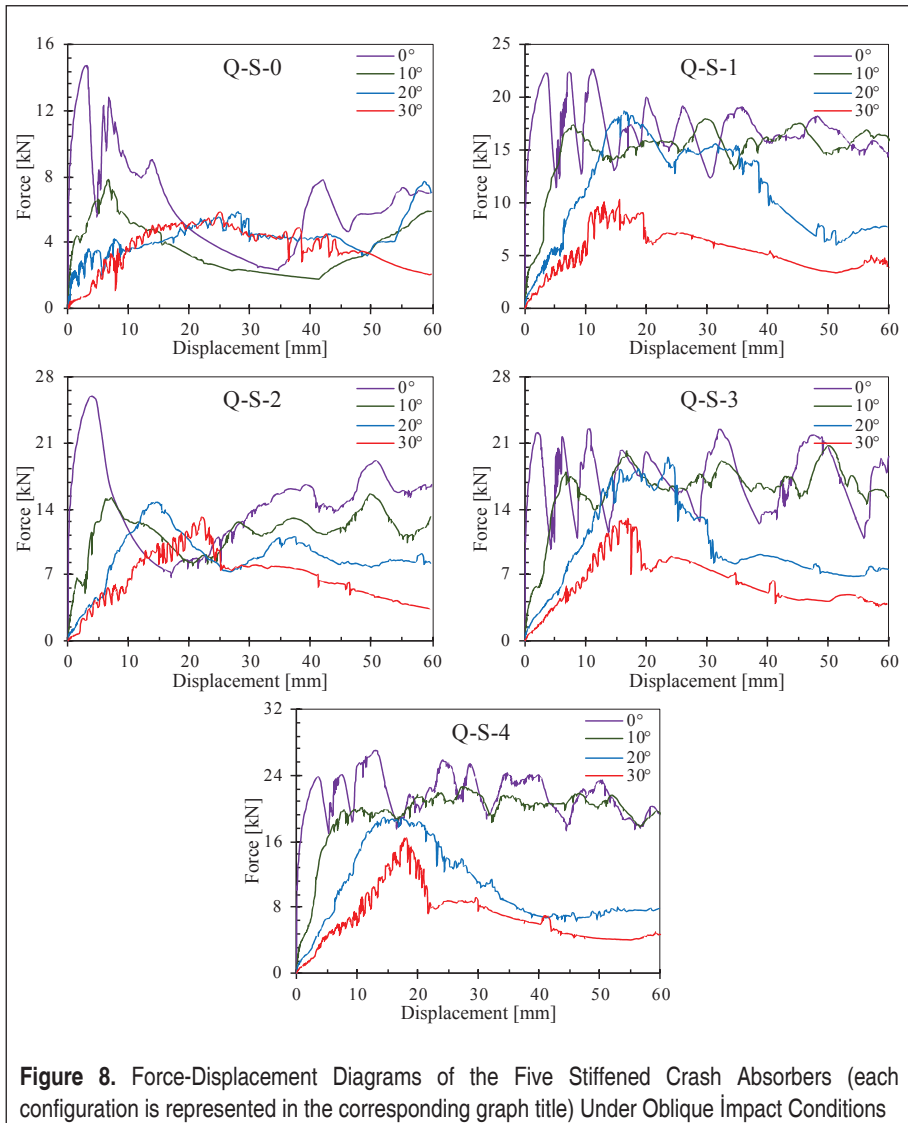


**Figure 8.** Force-Displacement Diagrams of the Five Stiffened Crash Absorbers (each configuration is represented in the corresponding graph title) Under Oblique Impact Conditions

that the performance indicators may change with the oblique impact angle. Therefore, it is a challenging task to decide an optimal tube profile that maintains crushing stability regardless of the impact angle. This finding indicates that a particular section profile should be proposed for superior crashworthiness performance depending on the impact angle. For example, the comparison between the Q-S-2 and the Q-S-4 is relatively complicated when the impact angle equals to 30° because Q-S-4 has slightly greater EA and SEA and a worse CFE and ULC value than the Q-S-2, as shown in

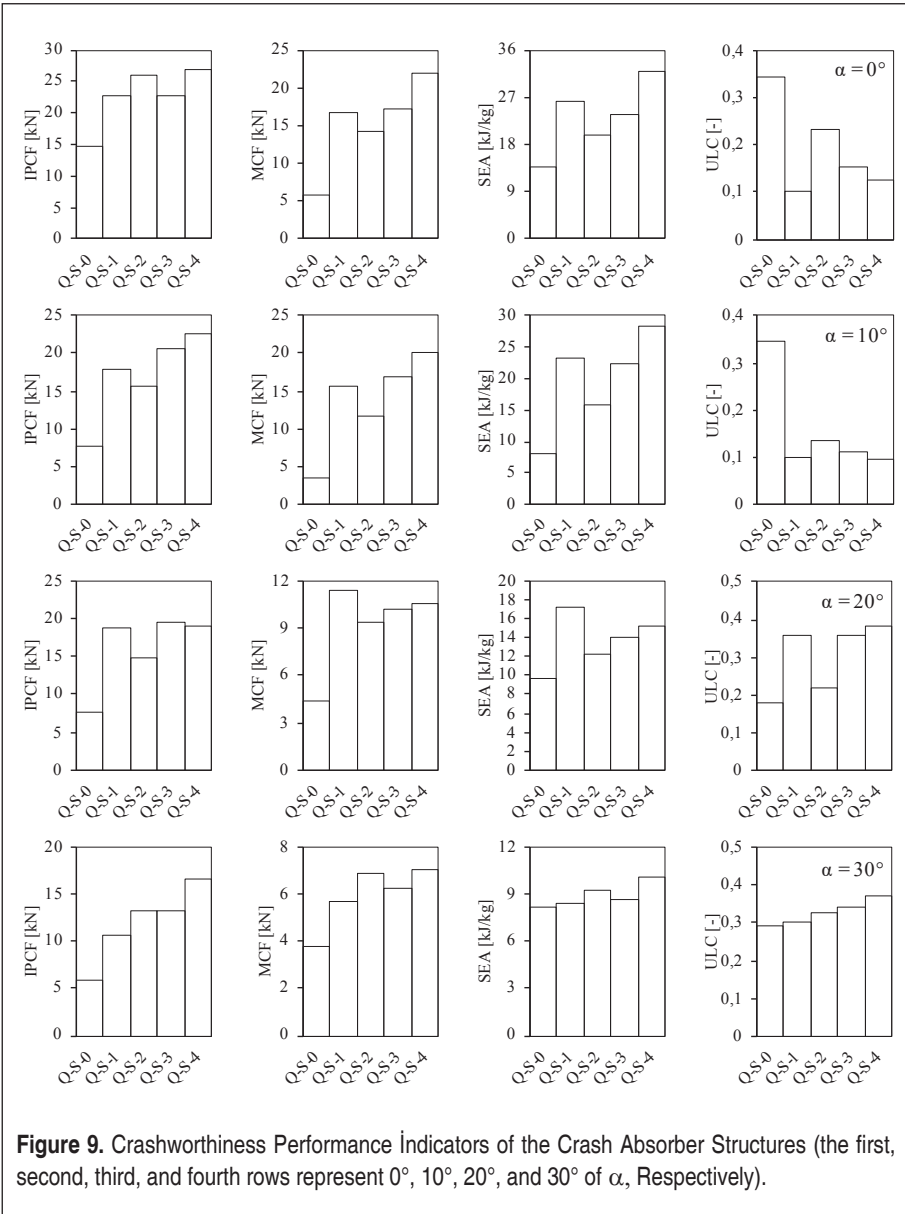


**Figure 9.** Crashworthiness Performance Indicators of the Crash Absorber Structures (the first, second, third, and fourth rows represent  $0^\circ$ ,  $10^\circ$ ,  $20^\circ$ , and  $30^\circ$  of  $\alpha$ , Respectively).

Table 3. It is noteworthy that the Q-S-4 experiences a small advantage in SEA and MCF, but a large disadvantage in IPCF and ULC. In this case, Q-S-2 type stiffener may be suggested as a more reliable crash absorber at higher impact angles if the occupant protection is of importance.



**Table 3.** Values of the Crashworthiness Performance Indicators of the Crash Absorbers Under Oblique Impact Conditions

		IPCF [kN]	MCF [kN]	EA [kJ]	SEA [kJ/kg]	ULC [-]
0°	Q-S-0	14.75	5.892	0.3765	13.9	0.342
	Q-S-1	22.78	16.79	1.0150	26.2	0.101
	Q-S-2	25.96	14.26	0.8621	19.7	0.231
	Q-S-3	22.64	17.25	1.0370	23.8	0.152
	Q-S-4	27.04	21.80	1.3050	31.8	0.127
10°	Q-S-0	7.838	3.505	0.2213	8.16	0.348
	Q-S-1	17.97	15.56	0.9044	23.3	0.099
	Q-S-2	15.63	11.75	0.6935	15.8	0.136
	Q-S-3	20.72	16.79	0.9727	22.3	0.111
	Q-S-4	22.69	20.08	1.1610	28.3	0.096
20°	Q-S-0	7.709	4.443	0.2613	9.63	0.182
	Q-S-1	18.77	11.41	0.6694	17.3	0.357
	Q-S-2	14.78	9.387	0.5382	12.3	0.218
	Q-S-3	19.51	10.16	0.6124	14.1	0.358
	Q-S-4	18.98	10.62	0.6258	15.2	0.384
30°	Q-S-0	5.887	3.734	0.2204	8.12	0.293
	Q-S-1	10.54	5.641	0.3268	8.43	0.302
	Q-S-2	13.29	6.846	0.4023	9.19	0.326
	Q-S-3	13.16	6.215	0.3762	8.64	0.343
	Q-S-4	16.55	6.989	0.4132	10.1	0.371

#### 4. CONCLUDING REMARKS

The present study aims to improve the crashworthiness performance of Al6061 tubes with quatrefoil sections under the oblique impact conditions by implementing four types of stiffener profiles through the dept of the tube geometry. The deformation patterns, the crashworthiness indicators, and the force-displacement diagrams are con-

sidered as a tool for selection of an ideal crash absorber stiffener profile that fits well with the quatrefoil section. The important results which can be drawn from the current study can be summarized as the followings:

- It is found that a progressive folding mechanism is almost obtained at axial and low impact angles ( $0^\circ$  and  $10^\circ$ ) whereas the stability of the collapse mechanism is disrupted at higher impact angles. It leads to a typical buckling behavior due to additional bending effects at higher impact angles thus the use of stiffener considerably reduces the risk of buckling and maintains load-bearing capacity in comparison with the unstiffened configuration Q-S-0.
- The oblique impact angle is found to be a severe impact in the shaping of force-displacement curves, which causes higher deviations in force history and lower energy absorption values. However, IPCF values drop sharply as the impact angle increases which may be pointed out as a positive effect in terms of occupant protection at the beginning of the crushing process.
- The crashworthiness performance indicators reveal that the Q-S-4 type of stiffener has a better design in comparison with the other stiffeners. However, it is quite difficult to make a generalization covering all of the impact angles because Q-S-1 is better than Q-S-4 at  $20^\circ$ . Furthermore, Q-S-2 emerges a better ULC value than Q-S-4 at  $30^\circ$ . To this end, the impact angle has a crucial role in the optimization of crash absorber structures thus cannot be disregarded in the design stage of such kinds of structures.

## ACKNOWLEDGEMENT

The authors are greatly thankful to Eskisehir Technical University, Turkey for providing the facilities in developing the paper. The authors have declared that no conflict of interests exists.

## REFERENCES

1. **Ying, L., Dai, M., Zhang, S., Ma, H., and Hu, P.** 2016. "Multiobjective crashworthiness optimization of thin-walled structures with functionally graded strength under oblique impact loading". *Thin-Walled Structures*, vol. 117, pp. 165–177.
2. **Alkhatib, S.E., Tarlochan, F., and Eyvazian, A.** 2017. "Collapse behavior of thin-walled corrugated tapered tubes". *Engineering Structures*, vol. 150, pp. 674–692.
3. **Fan, Z., Lu, G., Liu, K.** 2013. "Quasi-Static Axial compression of thin-walled tubes with different cross-sectional shapes". *Engineering Structures*, vol. 55, pp. 80–91.
4. **Tarlochan, F., Samer, F., Hamouda, A.M.S., Ramesh, S., Khalid, K.** 2013. "Design of thin wall structures for energy absorption applications: Enhancement of crashworthiness due to axial and oblique impact forces". *Thin-Walled Structures*, vol. 71, pp. 7–17.



5. **Liu, M., Zhang, L., Wang, P., Chang, Y.** 2015. "Buckling behaviors of section aluminum alloy columns under axial compression". *Engineering Structures*, vol. 95, pp. 127–137.
6. **Li, Z., Ma, W., Yao, S., Xu, P.** 2021. "Crashworthiness performance of corrugation-reinforced multicell tubular structures". *International Journal of Mechanical Sciences*, vol. 190, pp. 106038.
7. **Ma, W., Xie, S., and Li Z.** 2019. "Mechanical performance of bio-inspired corrugated tubes with varying vertex configurations". *Int. J. Mech. Sci.*, vol. 172, pp. 105399.
8. **Zhang, L., Bai, Z., and Bai F.** 2018. "Crashworthiness design for bio-inspired multi-cell tubes with quadrilateral, hexagonal and octagonal sections". *Thin-Walled Structures*, vol. 122, pp. 42–51.
9. **Xiang, X.M., Lu, G., and You, Z.** 2020. "Energy absorption of origami inspired structures and materials". *Thin-Walled Structures*, vol. 157, pp. 107130.
10. **Ha, N.S., Lu, G.** 2020. "A review of recent research on bio-inspired structures and materials for energy absorption applications". *Composites Part B: Engineering*, vol. 181, pp. 107496.
11. **Li, J., Zhang, Y., Kang, Y., Zhang, F.** 2021. "Characterization of energy absorption for side hierarchical structures under axial and oblique loading conditions". *Thin-Walled Structures*, vol. 165, pp. 107999.
12. **Tran, T.N.** 2020. "Study on the crashworthiness of windowed multi-cell square tubes under axial and oblique impact". *Thin-Walled Structures*, vol. 155, pp. 106907.
13. **Patel, S., Vusa, V.R., Guedes Soares C.** 2019. "Crashworthiness analysis of polymer composites under axial and oblique impact loading". *Int. J. Mech. Sci.*, vol. 156, pp. 221–234.
14. **Albak, E.İ.** 2021. "Crashworthiness design for multi-cell circumferentially corrugated thin-walled tubes with sub-sections under multiple loading conditions". *Thin-Walled Structures*, vol. 164, pp. 107886.
15. **Tarlochan, F., Samer, F., Hamouda, A.M.S., Ramesh, S., and Khalid, K.** 2013. "Design of thin wall structures for energy absorption applications: Enhancement of crashworthiness due to axial and oblique impact forces". *Thin-Walled Structures*, vol. 71, pp. 7–17.
16. **Lu, G. and Yu, T.X.** 2003. "Energy absorption of structures and materials". Elsevier.
17. **Guillow, S.R., Lu, G., Grzebieta R.H.** 2001. "Quasi-static axial compression of thin-walled circular aluminium tubes". *Int. J. Mech. Sci.*, vol. 43(9), pp. 2103–2123.
18. **Tang, Z., Liu, S., Zhang, Z.** 2013. "Analysis of energy absorption characteristics of cylindrical multi-cell columns". *Thin-Walled Struct.*, vol. 62, pp. 75–84.
19. **Baroutaji, A., Morris, E., Olabi, A.G.** 2014. "Quasi-static response and multi-objective crashworthiness optimization of oblong tube under lateral loading". *Thin-Walled Struct.*, vol. 82, pp. 262–277.
20. **Nia, A.A., Parsapour, M.** 2014. "Comparative analysis of energy absorption capacity of



simple and multi-cell thin-walled tubes with triangular, square, hexagonal and octagonal sections”, *Thin-Walled Struct.*, vol. 74, pp. 155–165.

21. **Pirmohammad, S., Marzdashti, S.E.** 2016. “Crushing behavior of new designed multi-cell members subjected to axial and oblique quasi-static loads”. *Thin-Walled Struct.*, vol. 108, pp. 291–304.
22. **Abramowicz, W., Wierzbicki, T.** 1989. “Axial crushing of multicorner sheet metal columns”. *J. Appl. Mech.*, vol. 56, pp. 113–120.
23. **Nia, A.A., Hamedani, J.H.** 2010. “Comparative analysis of energy absorption and deformations of thin walled tubes with various section geometries”. *Thin-Walled Struct.*, vol. 48, pp. 946–954.
24. **Tarlochan, F., Samer, F., A.M.S. Hamouda, A.M.S.** 2013. “Design of thin wall structures for energy absorption applications: Enhancement of crashworthiness due to axial and oblique impact forces”. *Thin-Walled Struct.*, vol. 71, pp. 7–17.
25. **Liu W.** 2016. “Dynamic performances of thin-walled tubes with star-shaped cross section under axial impact”. *Thin-Walled Struct.*, vol. 100, pp. 25–37.
26. **Abbasi, M.** 2015. “Multiobjective crashworthiness optimization of multi-cornered thin-walled sheet metal members”. *Thin-Walled Struct.*, vol. 89, pp. 31–41.
27. **Fan, Z., Lu, G., Liu, K.** 2013. “Quasi-static axial compression of thin-walled tubes with different cross-sectional shapes”. *Eng. Struct.*, vol. 55, pp. 80–89.
28. **Kocabaş İ., Yılmaz H.** 2021. “A Numerical Investigation on Crashworthiness Performance of Thin-Walled Tubular Sections”, 7. ULUSLARARASI MUHENDİSLİK MİMARLIK VE TASARIM KONGRESİ, 21-22 Mayıs 2021.
29. **Li, Z., Ma, W., Yao, S., and Xu, P.** 2020. “Crashworthiness performance of corrugation-reinforced multicell tubular structures”. *Int. J. Mech. Sci.*, vol. 190, pp. 106038.